Lateral Wave Breaking and "Shingle" Formation in Large-Scale Shear Flow

MELVIN E. STERN

Graduate School of Oceanography, University of Rhode Island, Narragansett, RI 02882

(Manuscript received 26 February 1985, in final form 25 April 1985)

ABSTRACT

The temporal evolution of large amplitude quasi-geostrophic disturbances in a piecewise uniform potential vorticity flow is elucidated by numerical solutions of the "contour dynamical" equations. Lateral wavebreaking occurs when the initial disturbance amplitude exceeds a certain value, and at later times tongues of the lower vorticity fluid are engulfed or entrained into the higher vorticity shear flow. The effect appears to be important for the evolution of "shingles" observed between the coastal water and the cyclonic side of the Gulf Stream. The effect may also be an important phase in initiating the mixing process at the perimeter of an eddy embedded in another water mass.

1. Introduction

The "engulfment" of relatively cool coastal water on the inshore edge of the Gulf Stream and the "backward" breaking of the warmer Gulf Stream water, as it wraps around the engulfed water, are familiar features of the Stream as it emerges from the Straits of Florida (Lee and Atkinson, 1983; Brooks and Bane, 1983). The first named reference documents this "shingle" structure in the near region of the Straits of Florida, while the second concentrates on the vicinity of the "Charleston Bump," where a topographic forcing mechanism is suggested. Although the initiation of the disturbance in the southern region might be due to a local barotropic–baroclinic instability, such a mechanism is not supported by measurements (Lee and Atkinson, 1983) that indicate transfer of disturbance energy to mean kinetic and potential energy. An alternative mechanism may be due to the finite amplitude and slowly varying downstream velocity fluctuations already present in the Straits of Florida. In the emerging flow the fast moving parcels tend to "catch up" with slower ones (Stern and Vorapayev, 1984; Stern and Pratt, 1985) thereby greatly increasing the transverse velocities. In any case, it seems reasonable to break the whole problem into two parts, one of which (considered herein) studies the evolution of given initial finite amplitude disturbances in a shear flow. (The other part, which studies the origin of the disturbance, is not considered herein.)

The evolutionary problem will be examined by the method of contour dynamics, which has been used previously to obtain solutions of the two-dimensional Euler equation for barotropic flows having piecewise uniform vorticity (Pullin, 1981; Stern and Pratt, 1985). The latter reference discussed the barotropic intrusion of the nose of a uniform vorticity current along a wall (coast) and into a surrounding irrotational fluid. Since this coast is on the wrong side of the stream (as far as the Gulf Stream shingle problem is concerned) we shall begin by removing all walls and by considering the barotropic model in Fig. 1a. We will call the semi-infinite irrotational region "coastal" water; also, the semi-infinite region of uniform vorticity will be identified with the inshore edge of the Gulf Stream in the generalization (Section 4) to follow. The barotropic model in Fig. 1b has equal and opposite vorticities on both sides of the front, whose undisturbed velocity profile is sketched on the right. (This barotropic model should be useful in future work on baroclinic Gulf Stream meanders involving both sides of the Stream.) The generalized model in Fig. 1c has arbitrary vorticities (q^+, q^-) on either side of the vorticity front.

We turn then (Section 4) to the more relevant oceanic model in which the effect of the vertical density stratification is incorporated by means of the well-known "equivalent" barotropic model (Fig. 1d). This consists of a heavy and dynamically passive layer lying beneath the shear flow in the upper layer. The latter, in turn, consists of two piecewise uniform potential vorticity regions separated by a vorticity front across which the velocity is continuous. When the downstream scale of the frontal disturbances is of the order of the radius of deformation and when the Rossby number is small, then the quasi-geostrophic approximation may be made. Attention is then directed to the case where the quasi-geostrophic potential vorticity is piecewise uniform.

The contour dynamical method used in the barotropic calculation is easily modified to apply to this case, and a nonlinear integro–differential equation for the frontal displacement $L(x, t)$ is obtained. This equa-

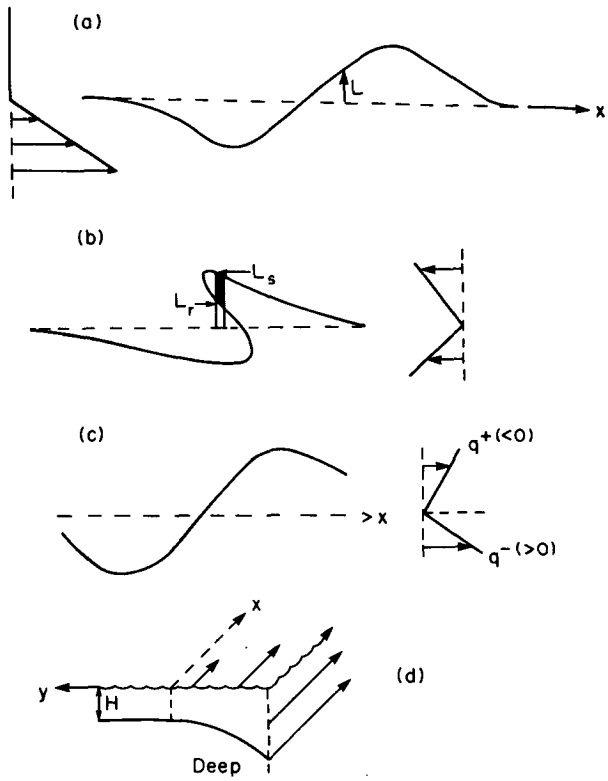

FIG. 1. (a) A barotropic flow in the horizontal x, y plane has uniform vorticity on one side of the front $y = L(x, t)$ and is irrotational on the other side. (b) As in (a) except that the vorticity above $y = L$ is equal and opposite to that below. Also, wavebreaking has occurred and L is multivalued. (c) As in (a) except the two vorticities (q^+, q^-) are arbitrary. L is drawn as single-valued. (d) Perspective sketch of the "equivalent" barotropic case. The undisturbed flow in the upper layer has piecewise uniform potential vorticity on either side of the x axis. This front is then displaced and the subsequent displacement is computed.

tion represents an enormous simplification of the inviscid dynamical problem because it reduces the number of spatial dimensions and it also eliminates the problem connected with the "tangling" of vorticity contours. We show that the numerical solutions for the equivalent barotropic model exhibit the same qualitative engulfment effect as the barotropic model, and thus we have high confidence in the relevance of the proposed mechanism for the oceanic "shingles." The more general significance of the engulfment effect in initiating the lateral mixing process at the edge of density fronts and isolated eddies is discussed in the last section.

2. Contour dynamics for piecewise uniform vorticity (barotropic) flow

The essence of the method used may be outlined as follows. Any infinitesimal element of area surrounding a point (x_1, y_1) and having a constant vorticity q will (by itself) produce a circular vortex in which the magnitude of the velocity decreases inversely with the radial distance r, and the corresponding streamfunction is proportional to $q \ln r$. The total streamfunction at a fixed point (x, y) is then obtained by summing the contribution from all the (x_1, y_1) points. Therefore, the position $L(x, t)$ of the contour curve separating the pieces of uniform vorticity determines the velocity at any point, and particularly on the contour. From this, the position $L(x, t + dt)$ can be predicted at a slightly later time, and by repetition we compute the contour at any finite later time. The mathematical formulation is as follows.

Consider first the case (Fig. 1c) where the displacement $L(x, t)$ from $y = 0$ (the dashed horizontal line) is single valued. Let $v = \partial\psi/\partial x$ be the y-velocity component, $u = -\partial\psi/\partial y$ the x-component, and ψ the streamfunction. Then, the piecewise constant vorticity $q = \nabla^2\psi$ is

$$q = \begin{cases} q^-, & y < L(x, t) \\ q^+, & y > L(x, t). \end{cases} \tag{2.1}$$

Let us define u_0, ψ_0, q_0 such that

$$\begin{gathered} u = u_0(y) + u', \quad \psi = \psi_0(y) + \psi', \\ u_0 = -\partial\psi_0/\partial y, \quad q = q_0 + q' \\ u_0 = \begin{cases} -yq^-, & y < 0 \\ -yq^+, & y > 0 \end{cases} \\ q_0 = \begin{cases} q^-, & y < 0 \\ q^+, & y > 0. \end{cases} \end{gathered} \tag{2.2}$$

Thus, it follows that $\nabla^2\psi' = q'$ where

$$q' = \begin{cases} q^- - q^+, & L > y > 0 \\ q^+ - q^-, & L < y < 0 \\ 0, & \text{otherwise.} \end{cases} \tag{2.3}$$

In Poisson's equation $\nabla^2\psi' = q'$, the contribution of the vortices between ξ and $\xi + d\xi$ to the streamfunction $\psi(x, y, t)$ is

$$\frac{d\xi}{4\pi}(q^- - q^+)\int_0^{L(\xi,t)} d\eta \ln(x - \xi)^2 + (y - \eta)^2, \quad L > 0$$

$$\frac{d\xi}{4\pi}(q^+ - q^-)\int_{L(\xi,t)}^{0} d\eta \ln(x - \xi)^2 + (y - \eta)^2, \quad L < 0.$$

In either case ($L \gtrless 0$) the total ψ' is

$$\psi'(x, y, t) = \frac{q^- - q^+}{4\pi}\int_{-\infty}^{+\infty} d\xi \int_0^{L(\xi,t)} d\eta \ln(x - \xi)^2 + (y - \xi)^2. \tag{2.4}$$

Equation (2.4) is valid even when L is multivalued (Fig. 1b) provided it is interpreted as an integral along the contour of L, with $d\xi$ being either positive or negative depending on the sign of the slope $\partial L/\partial\xi$. This remark can be verified by referring to Fig. 1b where the contribution to $\psi'(x, y, t)$ of the vorticies in the

shaded region between L_r and L_s is obviously equal to the left-hand side of

$$\frac{|d\xi|}{4\pi}(q^- - q^+)\int_{L_r}^{L_s}(\cdots)d\eta = \frac{|d\xi|}{4\pi}(q^- - q^+) \times \int_0^{L_s}(\cdots)d\eta - \frac{|d\xi|}{4\pi}(q^- - q^+)\int_0^{L_r}(\cdots)d\eta$$

(where the integrands are deleted for convenience). In this identity the first term on the right corresponds to the contribution to the *contour integral* (2.4) of the upper branch (Fig. 1b) along which $d\xi > 0$. The last term corresponds to the lower branch along which $d\xi < 0$, and thus we conclude that (2.4) is valid for all simply connected domains.

The value of u' for any point on the front is obtained by differentiating (2.4) with respect to $-y$, simplifying the result, and then setting $y = L(x, t)$. When $u_0(L)$ in (2.2) is added to u' we get the Lagrangian velocity

$$\frac{dx}{dt} = \begin{Bmatrix} -q^- L, & L < 0 \\ -q^+ L, & L > 0 \end{Bmatrix} + \frac{q^- - q^+}{4\pi} \times \int_{-\infty}^{+\infty} d\xi \ln \frac{(x-\xi)^2 + [L(x,t) - L(\xi,t)]^2}{(x-\xi)^2 + L^2(x,t)}. \quad (2.5)$$

Differentiation of (2.4) with respect to x and simplification gives $v = dL/dt$:

$$\frac{dL}{dt} = \frac{q^- - q^+}{4\pi}\int_{-\infty}^{+\infty} d\xi \frac{\partial L(\xi,t)}{\partial \xi} \times \ln\{(x-\xi)^2 + [L(x,t) - L(\xi,t)]^2\}. \quad (2.6)$$

The $y = 0$ level may be defined such that

$$\int_{-\infty}^{+\infty} L d\xi = 0 \quad (2.7)$$

initially, and mass conservation requires (2.7) to hold at all t.

For the case of Fig. 1a, where $q^+ = 0$ we may take $q^- = 1$ without loss of generality. This implies that the unit of time is the reciprocal of the vorticity, and the unit of length will be taken as the characteristic downstream width of the initial disturbance. The nondimensional Lagrangian equations then become

$$\frac{dx}{dt} = \begin{Bmatrix} -L, & L < 0 \\ 0, & L > 0 \end{Bmatrix} + \frac{1}{4\pi} \times \int_{-\infty}^{+\infty} d\xi \ln \frac{(x-\xi)^2 + [L(x,t) - L(\xi,t)]^2}{(x-\xi)^2 + L^2(x,t)} \quad (2.8)$$

$$\frac{dL}{dt} = \frac{1}{4\pi}\int_{-\infty}^{+\infty} d\xi \frac{\partial L}{\partial \xi} \times \ln\{(x-\xi)^2 + [L(x,t) - L(\xi,t)]^2\}. \quad (2.9)$$

The first of the two terms on the right of (2.8) may be interpreted as the effect of the undisturbed mean field in advecting a particle on the front. Acting alone this term would propagate each $L < 0$ with a speed equal to $|L|$, thereby causing the front to steepen and fold as discussed further. The remaining terms (integrals) in (2.8)–(2.9) may be interpreted as the velocities induced by vortex *anomalies* lying in the area between the $y = 0$ axis and the L curve. If $L(x, t)$ is locally positive, then the region just below the curve is filled with *positive* vortex anomalies (relative to the undisturbed mean field), and it is easy to see that these will tend to induce downward displacements of L at smaller x. The interpretation of subsequent numerical results is also helped by evaluating (2.8) for a steplike $L(x, 0)$ in which $L = +1$ for $0 < x < w$, and $L \to 0$ elsewhere. For x slightly greater than zero, Eq. (2.8) is negative, whereas (2.8) is positive for x slightly less than zero, and the difference is

$$u(x = 0^+, t = 0) - u(0^-, 0) = -\frac{1}{2\pi}\int_0^w d\xi \ln \frac{\xi^2 + 1}{\xi^2} \geqslant -\frac{1}{2}. \quad (2.10)$$

From this we conclude that a steep but finite positive slope ($\partial L/\partial x \gg 1$) will increase with time if $L > 0$, and wave breaking (with multivalued L) will occur a short time later. It is easily shown that at the other edge ($x = w$) of the step the magnitude of the slope decreases with time. For a negative step with $L(x, 0) = -1$ in $0 < x < w$ we find

$$u(w^+, 0) - u(w^-, 0) = -1 + \frac{1}{2\pi}\int_0^w \ln \frac{\xi^2 + 1}{\xi^2} d\xi \leqslant -\frac{1}{2}. \quad (2.11)$$

Thus we see that wave breaking occurs at $x = w$ for the negative L case, and it occurs faster than the positive L case. For further discussion of the time of wave breaking see Stern and Pratt (1985).

3. Numerical calculations

The integro–differential Eqs. (2.8)–(2.9) for the simple barotropic model were solved on an IBM PC using n Lagrangian points $x_1, \ldots, x_n$. The velocity components dx_i/dt, dL_i/dt were computed by using a trapezoidal approximation to the integrals (2.8)–(2.9), with indentations at the (integrable) singularities where analytical approximations were used. The program for the instantaneous velocities was checked by computing the result for a step function in $L(x, 0)$ and by comparison with the previously mentioned analytical result (2.10) for the front and back of the step. For $n = 65$, agreement was better than 1% except near the sharp corner of the step where the agreement was 7%. The runs described below were done with greater n and with smooth initial conditions. A second-order Runge-Kutta scheme was used in the temporal integration of an isolated disturbance: $L(\pm\infty, t) = 0 = (dx/dt)_{\pm\infty}$ and

these boundary conditions were imposed on the two finite endpoints (x_1, L_1), (x_n, L_n).

For the nondimensional initial condition

$$L(x, 0) = \frac{2Ax}{(1 + x^2)^2} \tag{3.1}$$

a preliminary check of the entire numerical program was obtained by using a small amplitude ($A = 0.01$) and by comparing the results with the analytic prediction of $L(x, t)$ obtained from elementary linear theory. It is easily verified from the latter that all x-sinusoidal waves propagate with the same frequency (one-half) (so that the group velocity vanishes for all wavelengths), and $L(x, t)$ is given by a linear combination of the Fourier sin/cos transforms of (3.1). One then finds that for $A > 0$ the minimum L (see Fig. 1a) propagates phase to larger x during the first half of the period ($2\pi/\frac{1}{2}$), but the maximum L does not propagate far because it is too near the end of the "group" and because the group velocity vanishes. Likewise the minimum L does not continue to propagate but is "reflected" from the leading edge of the group and subsequently transformed into a maximum L. This maximum then propagates phase backwards (as may be seen by sketching the analytical solution) until it is reflected at the rear of the group and thereby transformed into a minimum, which (at time $= 4\pi$) is identical to the initial condition. In the numerical test of our program at small amplitude we could see our fixed end point condition contaminating the result at large x when $t \sim 4\pi$, but the following runs were confined to much shorter time intervals so that no serious endpoint contamination arose. We also mention that (2.7) was satisfied in all runs (except one to be mentioned) so that the far-field (large x) velocities decrease like the field of a *dipole* field [cf. the positive and negative areas of (3.1)], as contrasted with the much larger monopole (point vortex) field which could occur if L had a finite area.

Figure 2a, b shows the temporal evolution for $A = 1$, $n = 85$, $x_1 = -5$, $x_n = 8$, $\Delta x = 0.05$, $\Delta t = 0.1$, where Δx is the typical distance between adjacent initial points (except near the endpoints where the spacing is greater) and Δt is the time step. The most striking effect at $t = 0.6$–1.2 is the steepening of the front, caused by the mean field advection of the minimum L [as given by the first of the two terms on the right of (2.8)]. For very small amplitude (A) min$L$ would phase propagate much slower and there would be no wave breaking. The post wavebreaking stage $t > 1.2$ can be qualitatively explained by the remarks made in connection with (2.11). Figure 2b shows the subsequent engulfment of irrotational water, in a way that resembles Fig. 21 of Lee and Atkinson (1983). Reversing the amplitude ($A = -1$) causes a notable difference at early times (Fig. 3a), because there is no "mean field contribution" to u for $L > 0$, and thus the crest at $L > 0$ does not move much. Also at these early times the minimum L weakens because of the dominant dispersive effects at the leading edge of the "group." At later times the front behind the quasi-stationary crest steepens in accord with the argument used in connection with (2.10), and wavebreaking then occurs (Fig. 3a). In addition to this steepening of the rear part of the crest, the cyclonic vortices therein induce a downward motion of the front at smaller x, so that the front there is displaced below the x axis as shown on the left-hand side of Fig. 3a. A trough is formed there that then comes under the influence of the mean field advection; this accounts for the engulfment effect shown in Fig. 3b. In this respect the net qualitative effect is similar to the $A = +1$ case.

One numerical calculation was done for a "monopole" initial field: $L(x, 0) = -\exp[-(4x/3)^2]$, which produces relatively large $O(1/x)$ interfacial displacements at large $|x|$. This increases the numerical problem at the endpoints and the mass or area (in $x_1 < x < x_n$) will not have the desirable conservative property. In the region (Fig. 4a) of wavebreaking, however, there is apparently no important local effect of the end errors on the engulfment that is qualitatively similar to Fig. 2b. The calculation has not been carried further because endpoint contamination is already visible in Fig. 4b and the bounded area between $x = -5$ and $x = 8$ is one-half of its original value.

The last barotropic case to be presented is that of a free isolated jet with $q^- = \frac{1}{2} = q^+$. The undisturbed state (Fig. 1c) consists of an anticyclonic shear flow for $y > 0$ and a cyclonic shear for $y < 0$. A simple inversion of the axis will transform the result to the more interesting geometry of a jet with a piecewise linear shear flow having maximum velocity on $y = 0$. When $q^- = \frac{1}{2} = q^+$, Eqs. (2.5)–(2.6) are identical to the previously considered models except for the mean field term in (2.5). Thus, only a small modification of the numerical program is necessary. For $A = +1$ [Eq. (3.1)], the result is given in Fig. 5. Since the mean velocities are positive on both sides of $y = 0$ and the dispersive effect is strong at the leading edge of the group (zero group velocity), breaking occurs in the trough for $A = +1$. Reversing the sign of A causes the crest to trail relative to the trough. Under the influence of the forward mean flow, the crest would also break in the forward direction. If the diagram is rotated 180° about the L axis (Fig. 5) so that the mean flow for $|y| > 0$ is moving to the right slower than the observer, then an observer moving with (and looking in the same direction as) the maximum undisturbed jet velocity would see "backward" breaking waves.

4. The equivalent barotropic model

Does the engulfment effect occur in more realistic oceanic models, such as including density variations? The simplest generalization of the foregoing is the equivalent barotropic model (Fig. 1d) consisting of a very deep and dynamically passive (except for the re-

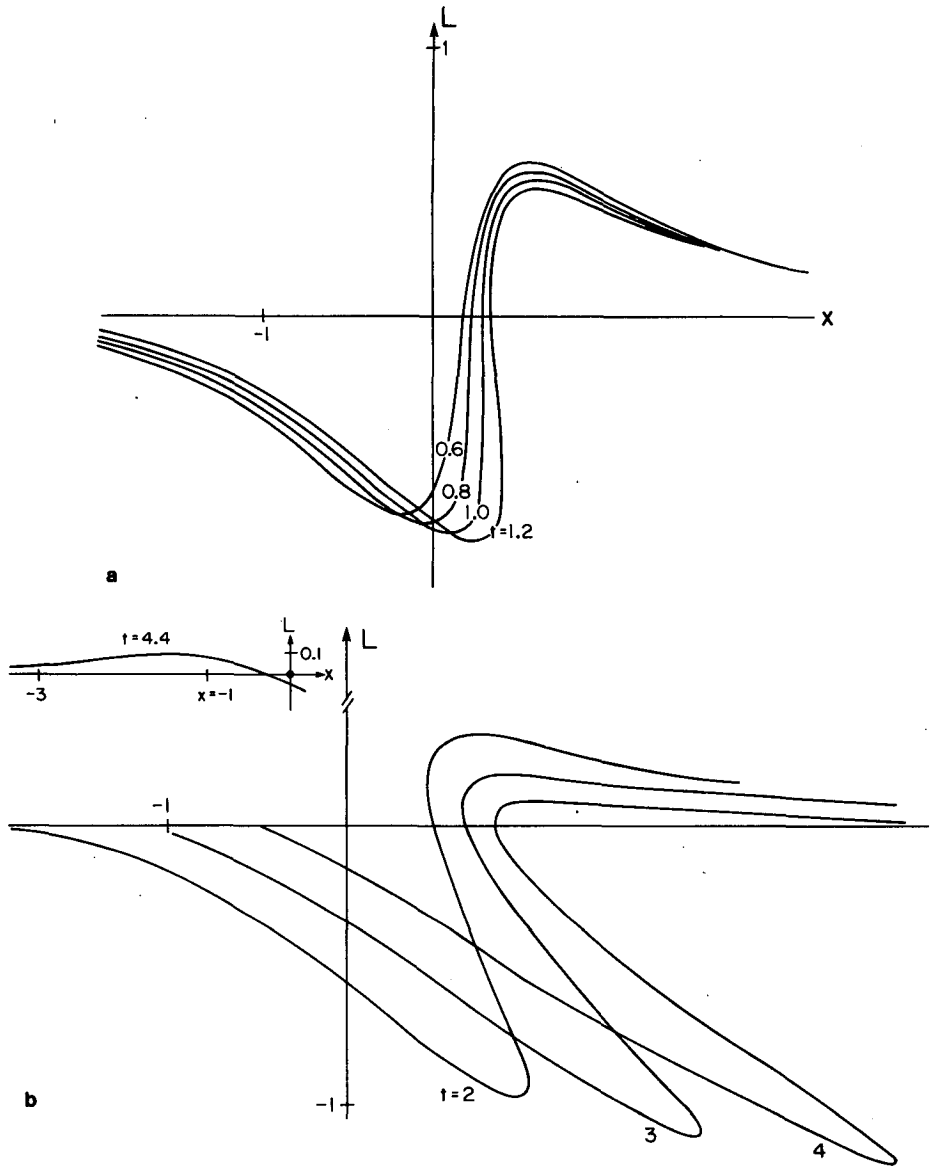

FIG. 2. The temporal evolution corresponding to Fig. 1a when the amplitude $A = 1$. (a) The trailing trough propagates faster than the ridge and wavebreaking occurs at $t = 1.2$. (b) The subsequent evolution showing engulfment of the irrotational fluid. The inset (left) is an enlargement of the trailing edge of the disturbance at $t = 4.4$.

duced value of gravity) layer beneath a lighter layer. We will subsequently assume that the latter consists of two semi-infinite domains of uniform potential vorticity, with $y = L(x, t)$ denoting the nondimensional displacement of the front. The Rossby radius of deformation, based on the vertical layer thickness at $y = \infty$ (Fig. 1d), supplies the length unit, and the reciprocal of the vorticity jump across the undisturbed front supplies the time unit in the following nondimensional equations. These units then determine the scale for the geostrophic velocity $\mathbf{v} = \mathbf{k} \times \nabla h$, where h is the departure of the layer thickness from the value at infinity [i.e., $h(x, \infty, t) = 0$] and $\mathbf{k}$ is the unit vertical vector. The Rossby number is assumed small and the downstream length scale is assumed O(1); thus, we obtain the well-known quasi-geostrophic vorticity approximation:

$$(\partial/\partial t + \mathbf{v} \cdot \nabla)(\nabla^2 h - h) = 0 \tag{4.1}$$

$$\mathbf{v} = \mathbf{k} \times \nabla h. \tag{4.2}$$

The highly nonlinear problem (4.1)–(4.2) is greatly simplified by stipulating (as mentioned previously) that the conserved potential vorticity $\nabla^2 h - h$ is also piece-

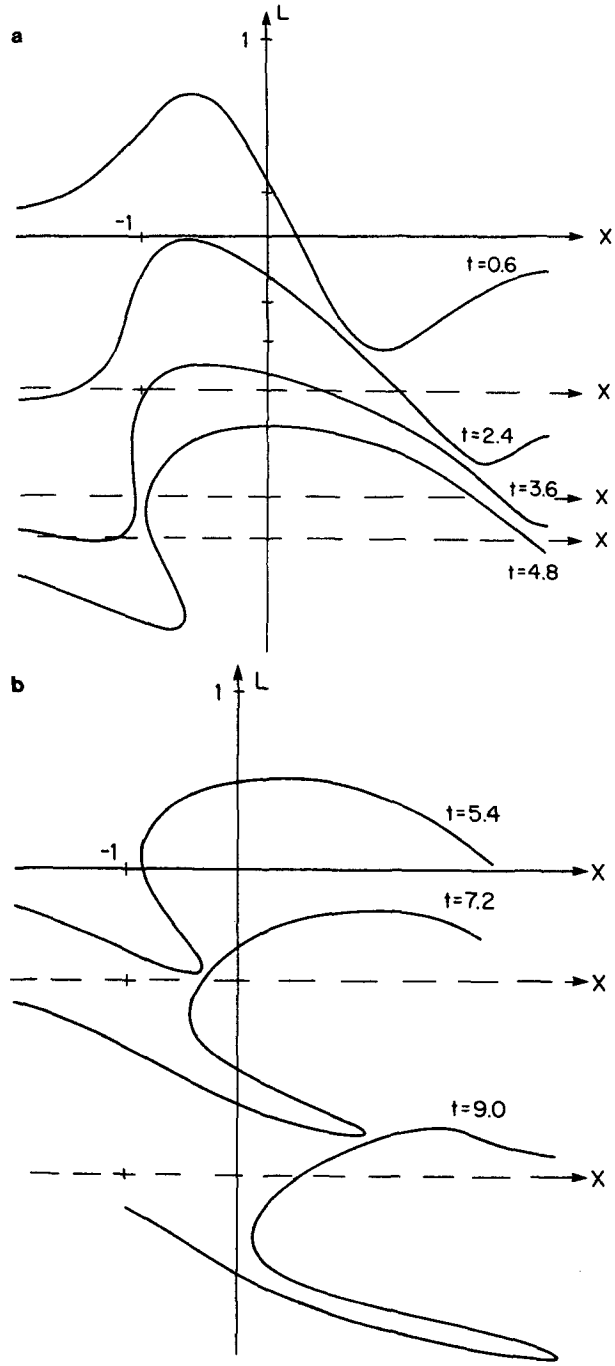

FIG. 3. As in Fig. 2 except $A = -1$. The curves at different times are offset. (a) Note the trailing ridge in this case remains nearly stationary and wavebreaking occurs behind it. (b) Later time showing engulfment.

wise uniform. Without loss of generality for the geometry of Fig. 1d, we then have

$$\nabla^2 h - h = \begin{cases} 0, & y > L(x,t) \\ 1, & y < L(x,t). \end{cases} \tag{4.3a}$$

For obvious procedural reasons we want to consider a model which formally reduces to Fig. 1a when the lateral scale of the disturbance $L(x, t)$ is small compared to the radius of deformation. Accordingly we consider the model whose undisturbed ($L = 0$) state, denoted by $h = h_0(y)$, $\mathbf{v} = \mathbf{v}_0(u_0(y), 0)$, is given by

$$h_0 = \begin{cases} 0, & y > 0 \\ (\cosh y) - 1, & y < 0, \end{cases} \qquad u_0 = \begin{cases} 0 & y > 0 \\ -\sinh y, & y < 0. \end{cases} \tag{4.3b}$$

This undisturbed state has uniform dimensional thickness (H in Fig. 1d) for $y > 0$ and the basic flow starts to increase linearly with negative y. While it is true that u_0 continually increases with $-y$, this artificiality is not of major concern in application to the Gulf Stream shingle problem because the velocity perturbations caused by $L(x, t)$ only extend a radius of deformation from the front.

Following the procedure used previously, we let $h = h_0(y) + h'(x, y, t)$, $u' = -\partial h'/\partial y$, $u = u_0(y) + u'$, $v = \partial h'/\partial x$. Since $\nabla^2 h_0 - h_0$ is unity for $y < 0$ and zero for $y > 0$, Eq. (4.3a) becomes

$$\nabla^2 h' - h' = \begin{cases} -1, & L(x,t) < y < 0 \\ +1, & L > y > 0 \\ 0, & \text{otherwise.} \end{cases} \tag{4.3c}$$

Since $h' = 0$ at $x = +\infty$, the Green's function for this problem is the Bessel function K_0 of the second kind. Therefore, the solution of (4.3c) is

$$h'(x, y, t) = -\frac{1}{2\pi} \int_{-\infty}^{+\infty} d\xi \int_0^{L(\xi,t)} d\eta \times K_0[(x-\xi)^2 + (y-\eta)^2]^{1/2} \tag{4.4}$$

for all simply connected L. Evaluating $v = \partial h'/\partial x$ and $u = u_0 - \partial h'/\partial y$ on $y = L(x, t)$ then gives the contour dynamical equations

$$\frac{dx}{dt} = \begin{Bmatrix} 0, & L > 0 \\ -\sinh L, & L < 0 \end{Bmatrix} - \frac{1}{2\pi} \int_{-\infty}^{+\infty} d\xi \{K_0[(x-\xi)^2 + (L(x,t) - L(\xi,t)^2]^{1/2} - K_0[(x-\xi)^2 + L^2(x,t)]^{1/2}\} \tag{4.5}$$

$$\frac{dL}{dt} = -\frac{1}{2\pi} \int_{-\infty}^{+\infty} d\xi \frac{\partial L(\xi,t)}{\partial \xi} \times K_0\{(x-\xi)^2 + [L(x,t) - L(\xi,t)]^2\}^{1/2}. \tag{4.6}$$

Since $K_0(r) \to -\ln r$ as $r \to 0$, it is readily seen that these equations reduce to (2.8)–(2.9) when the scale and amplitude of L are $\ll 1$ (i.e., small compared to the radius of deformation). Also of interest is the velocity on $y = 0$:

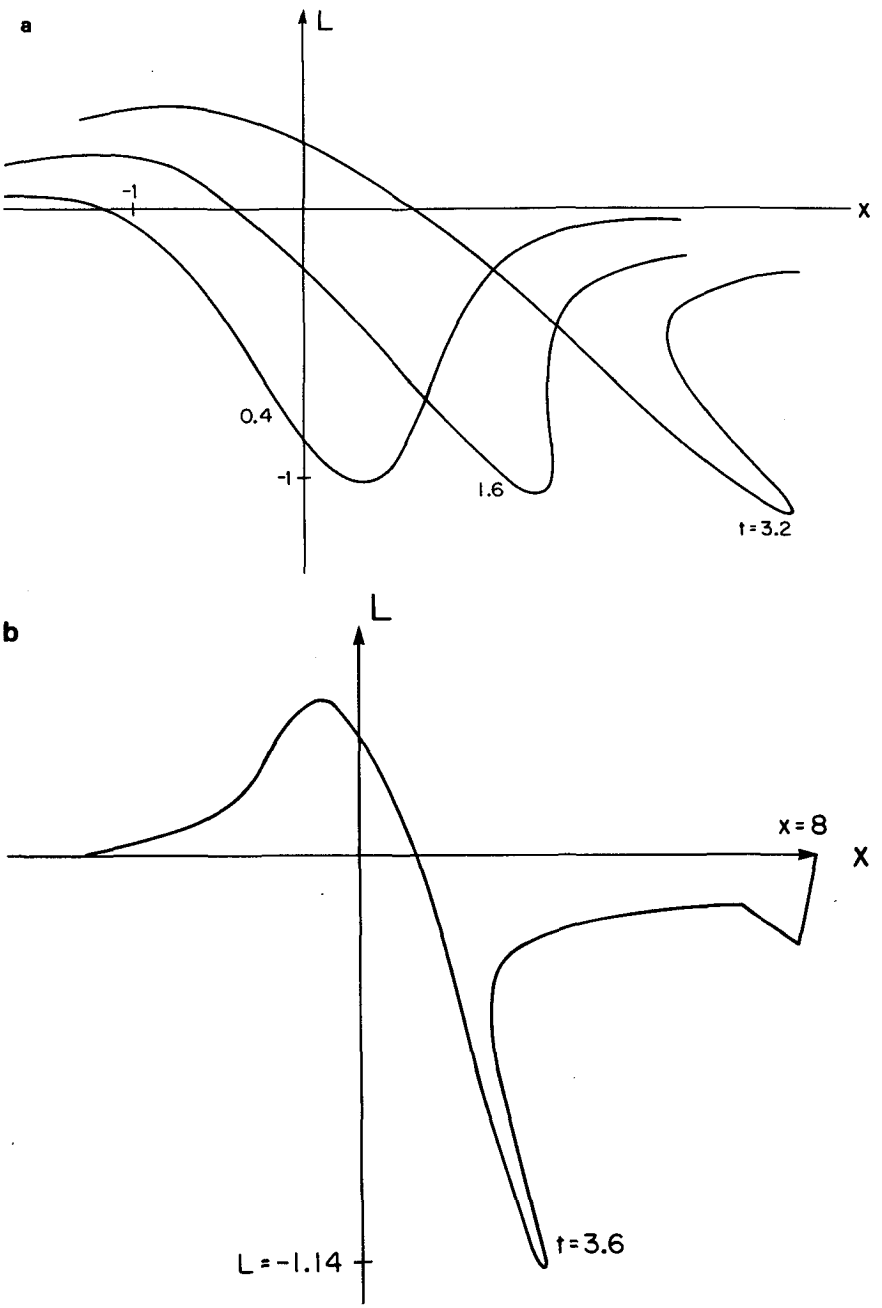

FIG. 4. (a) Evolution of a Gaussian $L(x, 0)$ (b) End of the calculation, showing contamination due to the right-hand boundary condition.

$$u(x, 0, t) = -\frac{1}{2\pi}\int_{-\infty}^{+\infty} d\xi K_0[(x-\xi)^2 + L^2(\xi, t)]^{1/2} + \frac{1}{2} \geqslant 0 \quad (4.7a)$$

$$\int_{-\infty}^{+\infty} u(x, 0, t)dx = \frac{1}{2}\int_{-\infty}^{+\infty} (1 - e^{-|L(\xi,t)|})d\xi \quad (4.7b)$$

where the identity (cf. Morse and Feshbach, 1953, p. 1324)

$$\frac{1}{\pi}\int_{-\infty}^{+\infty} K_0(z^2 + \lambda^2)^{1/2}dz = e^{-|\lambda|} \quad (4.7c)$$

has been used.

Despite the similarity of (4.5)–(4.6) to the barotropic equations (2.8)–(2.9) there are two notable differences.

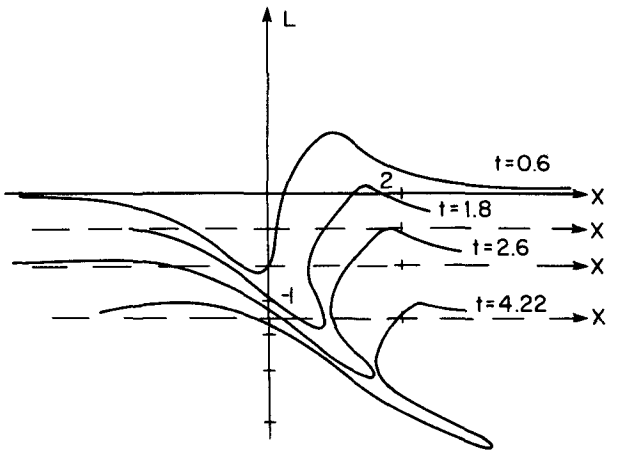

FIG. 5. Evolution of a trough and ridge disturbance for the case of Fig. 1c.

First, the influence of distant vorticies on a fixed x-point is much weaker due to the exponential decay of K_0. Second, the downstream propagation of energy is much more effective in the equivalent barotropic model as is partially revealed by the following "long-wave" approximation to (4.5)–(4.6). If at any time $L(x, t)$ varies slowly with x (on the scale of the radius of deformation) so that

$$|L(\xi, t) - L(x, t)|^2 \equiv O(\epsilon^2) \ll 1,$$

for

$$|x - \xi| = O(1),$$

then $\partial L/\partial x = O(\epsilon)$, $L(x, t) = O(1)$, and therefore,

$$v = \frac{dL}{dt} = \frac{\partial L}{\partial t} + u\frac{\partial L}{\partial x}$$

$$\approx -\frac{2}{2\pi}\frac{\partial L(x, t)}{\partial x}\int_0^\infty dz K_0(z) + \cdots$$

$$u = \frac{dx}{dt} \approx \begin{Bmatrix} 0 \\ -\sinh L \end{Bmatrix}$$

$$-\frac{1}{\pi}\int_0^\infty dz\{K_0(z) - K_0[z^2 + L^2(x, t)]^{1/2}\} + O(\epsilon).$$

In the $\epsilon \to 0$ limit, we have the long wave evolutionary equation

$$\partial L/\partial t + c(L)\partial L/\partial x = 0$$

$$c(L) = \begin{Bmatrix} 0, & L > 0 \\ -\sinh L, & L < 0 \end{Bmatrix}$$

$$+\frac{1}{\pi}\int_0^\infty dz K_0[z^2 + L^2(x, t)]^{1/2}$$

$$= \frac{1}{2}e^{-L}, \quad \text{all } L. \tag{4.8}$$

The well-known solution of (4.8) implies that a trough $L < 0$ propagates faster than a ridge and the *continually steepening* part of the front rotates in the same (cyclonic) sense as the shear of the mean flow. This (nonlinear long-wave) effect does not occur in the barotropic model (Section 3) because the group velocity (of linear waves) vanishes, and thus the breaking in the barotropic case is entirely due to short wavelength effects. Thus, we might expect that the latter will enhance the long wave tendency (4.8) for waves to break in the trough. Before demonstrating this, we remark that (4.8) has interesting implications for the *origin* (see the Introduction) of the disturbances which eventually fold into shingles. It is well known that large amplitude and slow temporal variations in downstream velocity exist in the Straits of Florida. By applying a long-wave theory such as Eq. (4.8) to the flow emerging from these confines, we see how the small cross-stream velocity components can be amplified (at the expense of downstream kinetic energy) as the wavefront steepens downstream. (See Stern and Vorapayev, 1984.)

Attention is therefore directed to the evolution of $L(x, 0)$ disturbances whose slope already is O(1); the type (2.12) was used for most of the calculations in order to compare the results with the previous barotropic model. We start with the moderately large amplitude $A = 1$ (Fig. 6) showing an evolution which is qualitatively similar to the barotropic case (Fig. 2a, b). Increasing the initial amplitude to $A = 2$ (Fig. 7) decreases the time of initial wavebreaking by a factor of two, but the qualitative aspect of engulfment of low potential vorticity fluid is the same. Decreasing the initial amplitude from $A = 1$ to $A = 0.5$ only produces a small increase in the time of initial wavebreaking (Fig. 8), but the amount of fluid engulfed (e.g., compare $t = 6$) is significantly less. The trend towards decreased engulfment is further demonstrated by Fig. 9 for the

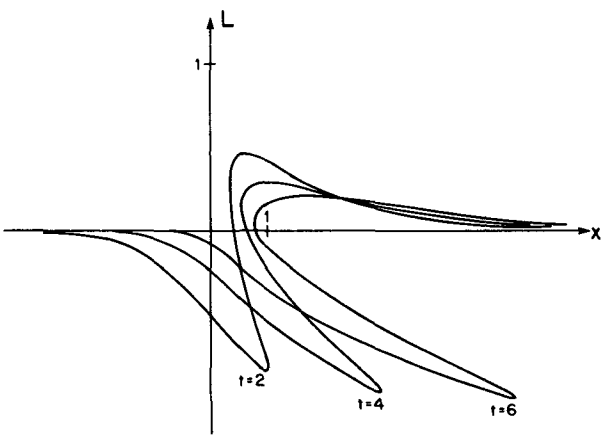

FIG. 6. Evolution of a trough and ridge disturbance for the case of the equivalent barotropic model (Fig. 1d). $A = 1$, time step = 0.1.

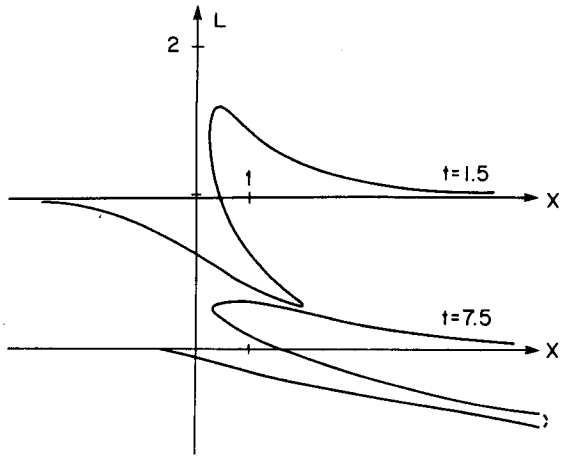

FIG. 7. As in Fig. 6 except larger amplitude ($A = 2$) and smaller time step.

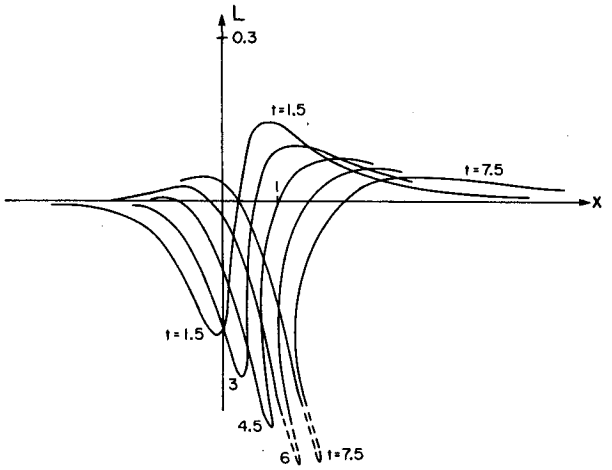

FIG. 9. As in Fig. 8 except smaller amplitude ($A = 0.3$).

initial amplitude $A = 0.3$. Finally, when $A = 0.15$ (Fig. 10) there is no wavebreaking and no engulfment. Figure 11 is a calculation for a different shape, *viz.* $L(x, 0) = \exp(-x^2)$. For this case we have a cyclonic "anomaly" lying above $y = 0$ and consequently initially uninfluenced by the "mean field term." The cyclonic anomaly is responsible for the negative L (see $t = 2$ in Fig. 11, for example) for reasons mentioned previously. These negative L then come under the influence of the mean field, thereby accounting for the wavebreaking and subsequent engulfment (Fig. 11). As a check on the conservation of mass (in $x_1 < x < x_n$) we found that the area bounded by $L(y, t)$ equals 1.774, 1.776, 1.774, 1.767, 1.741, 1.679 at the respective times: 0, 2, 4, 6, 8, 10. (In this quasi-geostrophic theory it is easy to show that the total area in $-\infty < x < \infty$ is conserved.)

Although the initial width (relative to the radius of deformation) of all these disturbances could have been systematically varied, it was not because we know the behavior when that width is small (Section 3) or when it is large (4.8).

5. Conclusions

We have shown that sufficiently large amplitude disturbances on the front separating fluid of low relative vorticity fluid from one with large shear (e.g., the cyclonic side of the Gulf Stream) will lead to wavebreaking and the engulfment of the low vorticity fluid into the shear flow. Over longer periods of time the shear flow "stretches" the engulfment into a long thin lense.

The initial amplitude in Fig. 8 is such that wave breaking is just marginal, and we see that the engulfed fluid occupies a very small area in a very thin tail.

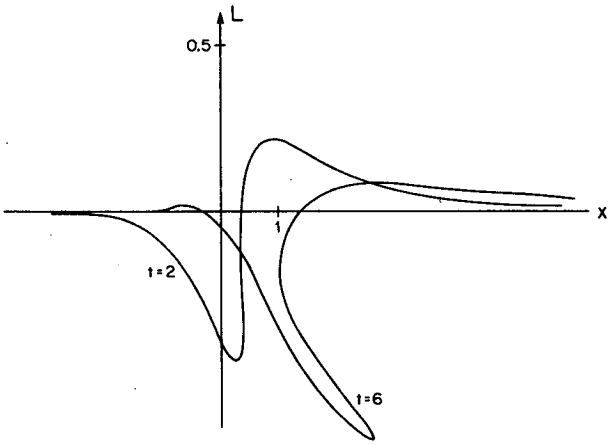

FIG. 8. As in Fig. 6 except smaller amplitude ($A = 0.5$).

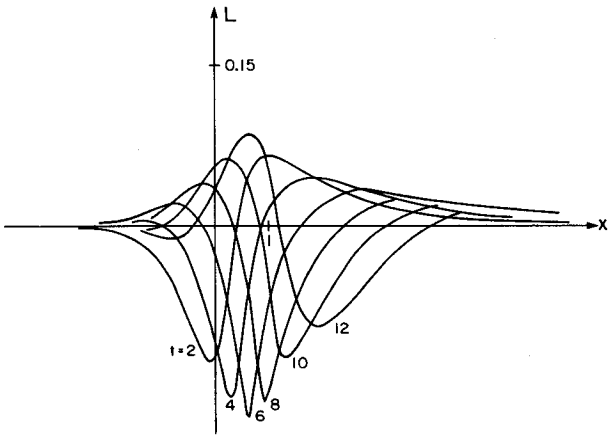

FIG. 10. As in Fig. 9 except smaller amplitude ($A = 0.15$).

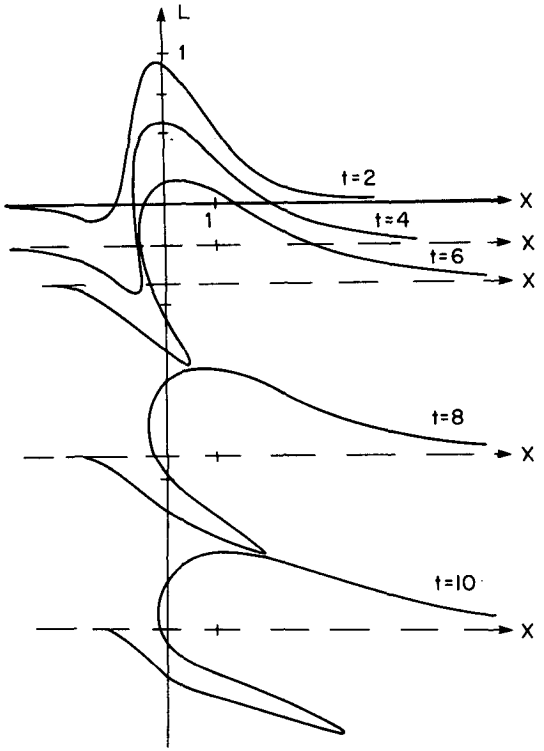

FIG. 11. Gaussian initial $L(x, 0) = \exp(-x^2)$. Note the rapid evolution of negative L.

From a dynamical point of view this appears inconsequential. If we take the liberty of merely "erasing" this tail, we are left with a simple $L(x, 6)$ which obviously has much smaller amplitudes than $L(x, 0)$. It is almost certain therefore that the disturbance energy has decreased with time, and this surmise is supported by estimates of horizontal velocities based on (4.7a) and (4.7b). Unfortunately, we did not program the detailed calculations necessary to verify the surmise (and the concomittant transfer of energy back into the mean flow) because our main interest was in the following thermodynamic significance of the problem.

We might regard the vorticity front as separating two continuously varying water masses, and these might even have different temperature and salinity provided they were density compensating. Although these fields are conservative with respect to motions of large (radius of deformation) scale, the engulfment effect (Fig. 6) will increase the horizontal temperature gradient and bring the water masses into such close contact that small-scale mixing processes (e.g., double diffusion) are effectively initiated. The enhanced diffusion thereby produced in the tail will leave a finite isolated thin lense completely entrained in the shear flow. Without the engulfment stage this effective means of mixing the two water masses would not have occurred. This speculative suggestion seems to be supported by the long thin detached filaments of coastal water found embedded in the thermocline of the Gulf Stream at very large distances downstream from their point of origin (Ford *et al.*, 1952).

The same engulfment mechanism might be operative at the perimeter of a large ocean eddy outside of which the relative vorticity is small. Mesoscale wavelets (perhaps due to a piecewise extremum in potential vorticity) on the circumference might break, forming thin lenses of water which are entrained inside the eddy in a way similar to that discussed above for the case of a rectilinear mean flow.

Acknowledgments. Partial support by the Office of Naval Research is gratefully acknowledged.

REFERENCES

Brooks, D. A., and J. M. Bane, 1983: Gulf Stream meanders off North Carolina during winter and summer 1979. *J. Geophys. Res.*, **88,** 4633–4650.

Ford, W. L., J. R. Longard and R. F. Banks, 1952: On the nature, occurrence, and origin of cold low salinity water along the edge of the Gulf Stream. *J. Mar. Res.*, **11,** 281–293.

Lee, T. N., and L. P. Atkinson, 1983: Low frequency current and temperature variability from Gulf Stream frontal eddies and atmospheric forcing along the southeast U.S. outer continental shelf. *J. Geophys. Res.*, **88,** 4541–4567.

Morse, P. M., and H. Feshbach, 1953: *Methods of Theoretical Physics.* McGraw-Hill, 1324–1325.

Pullin, D. I., 1981: The nonlinear behavior of a constant vorticity layer at a wall. *J. Fluid Mech.*, **108,** 401–421.

Stern, M. E., and S. I. Vorapayev, 1984: Formation of vorticity fronts in a shear flow. *Phys. Fluids,* **27,** p. 848.

——, and L. J. Pratt, 1985: Dynamics of vorticity fronts. *J. Fluid Mech.*, (in press).